Investigation on Parameters Affecting the Effectiveness of Photocatalytic Functional Coatings to Degrade NO: TiO2 Amount on Surface, Illumination, and Substrate Roughness

Julie Hot, Jivko Topalov, Erick Ringot, Alexandra Bertron

Hindawi
International Journal of Photoenergy
Volume 2017, Article ID 6241615, 14 pages
https://doi.org/10.1155/2017/6241615

Research Article

Investigation on Parameters Affecting the Effectiveness of Photocatalytic Functional Coatings to Degrade NO: TiO_2 Amount on Surface, Illumination, and Substrate Roughness

J. Hot,[1] J. Topalov,[1] E. Ringot,[1,2] and A. Bertron[1]

[1]*LMDC, INSA, UPS, Université de Toulouse, Toulouse, France*
[2]*LRVision, 13 rue du Développement, 31320 Castanet-Tolosan, France*

Correspondence should be addressed to J. Hot; hot@insa-toulouse.fr

Received 8 May 2017; Revised 22 July 2017; Accepted 2 August 2017; Published 24 September 2017

Academic Editor: Elisa Isabel Garcia-Lopez

This paper deals with the degradation of NO by photocatalytic oxidation using TiO_2-based coatings. Tests are conducted at a laboratory scale through an experimental setup inspired from ISO 22197-1 standard. Various parameters are explored to evaluate their influence on photocatalysis efficiency: TiO_2 dry matter content applied to the surface, nature of the substrate, and illumination conditions (UV and visible light). This article points out the different behaviors between three kinds of substrates which are common building materials: normalized mortar, denser mortar, and commercial wood. The illumination conditions are of great importance in the photocatalytic process with experiments under UV light showing the best results. However, a significant decrease in NO concentration under visible light is also observed provided that the TiO_2 dry matter content on the surface is high enough. The nature of the substrate plays an important role in the photocatalytic activity with rougher substrates being more efficient to degrade NO. However, limiting the roughness of the substrate seems to be of utmost interest to obtain the highest exposed surface area and thus the optimal photocatalytic efficiency. A higher roughness promotes the surface contact between TiO_2 and NO but does not necessarily increase the photochemical oxidation.

1. Introduction

Air pollution constitutes one of the main issues in urban areas where traffic pollutants such as nitrogen oxides (NO_x) are concentrated. Nitrogen oxides generally refer to two major species: nitric oxide (NO) and nitrogen dioxide (NO_2). They are widespread gaseous pollutants which have a direct impact on the global environment (acid rain formation) and human health (respiratory symptoms such as emphysemas, bronchitis) [1, 2]. Therefore, limiting the amount of NO_x in outdoor and indoor environments is an important and necessary priority for modern society [3–5]. Indoor air is indeed contaminated by a variety of toxic and hazardous substances as well as biological pollutants which have the potential to diminish the life quality of occupants and to pose serious health risks [6–8]. NO_x infiltrate in living areas from outdoor air pollution and are produced by domestic combustion appliances such as gas burners for cooking [9, 10].

During the last decade, the photocatalytic oxidation of NO_x emissions has attracted particular attention and has proven to be an efficient process. By using a photocatalytic material, atmospheric oxygen, water, and UV illumination, NO_x oxidation is easily promoted [11]. The semiconductor titanium dioxide (TiO_2) is the most widely used photocatalyst for environmental purification and especially water treatment and air cleaning. As TiO_2 in the form of anatase has a gap energy around 3.2 eV, its chemical activation illustrated in Figure 1 is provided under UV illumination ($\lambda < 388$ nm) and leads to the creation of electron-hole pairs (e^--h^+; cf. Figure 1, reaction 1). The pairs of mobile charges produced can reach the surface of TiO_2 particles and initiate oxidation-reduction reactions (cf. Figure 1, reactions 2 to 6). Holes h^+ react with OH^- ions or adsorbed H_2O present on the surface (cf. Figure 1, reactions 3 and 4) and electrons e^- reduce adsorbed O_2 (cf. Figure 1, reaction 5) yielding highly reactive species—hydroxyl radical ($OH^\bullet$), hydroperoxyl

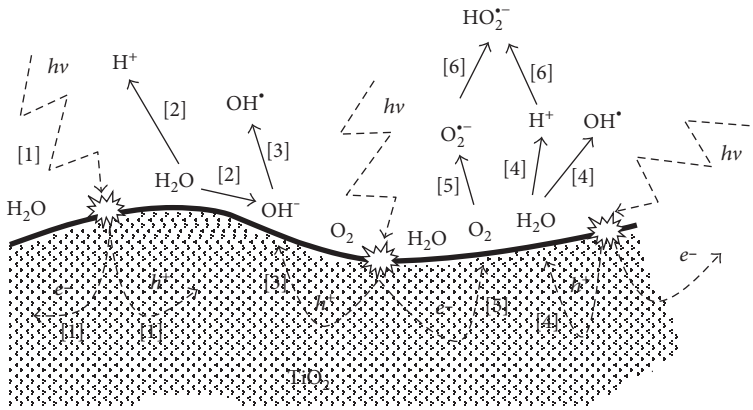

Figure 1: Chemical activation of TiO_2 under UV light: electron-hole pair creation and oxidation-reduction reactions.

radical ($HO_2^{\bullet}$), and superoxide anion ($O_2^{\bullet-}$)—which have the potential to decompose or mineralize a wide range of compounds [12–14].

Nitric oxide (NO) can be photocatalytically oxidized over titanium dioxide catalyst using hydroxyl and hydroperoxyl radicals according to the reactions 7 to 10 presented in Figure 2. The degradation of NO happens in two steps: the oxidation of NO to NO_2 which, in turn, reacts with $OH^{\bullet}$ and produces nitrite and nitrate ions NO_2^-/NO_3^- [15–17].

In recent years, many studies in the literature have been devoted to understand and improve the degradation of NO_x by photocatalysis using TiO_2-containing materials (TiO_2 is used as an additive and mixed with cement and concrete) or TiO_2-based dispersions (TiO_2 is used as a coating such as glaze and paint). Focus has especially been made on the NO_x photocatalytic oxidation mechanism [15, 18], the factors affecting the photocatalysis process [19–22], the experimental setup at a laboratory scale [23–28], and the development of photocatalysts active under visible light and the photocatalysis efficiency at real scale [29–35].

Results have shown that making building materials photoactive through the application of TiO_2 is a promising approach for solving the problems caused by nitrogen oxides. However, the reported photocatalytic degradation efficiency may vary from one study to another depending on the experimental conditions and the scale of the experiment. The air purification ability of TiO_2 is commonly studied at laboratory scale using flow-type reactors with different geometries and modes of operation simulating various environmental parameters [15, 16, 20, 23, 36]. A consensus between researchers was established, and a standardized experimental apparatus was defined to allow the performance of photocatalytic samples to be compared and also to identify the important parameters coming into play [5, 25, 26]. However, the transition of laboratory test results towards large scale applications remains critical. Indeed, the small size of flow reactor and the experimental conditions used at laboratory scale are not representative of real-world conditions and can lead to an overestimation of the photocatalytic efficiency [33]. As the photocatalysis process in the field environment is a trickier task, less studies deal with the degradation of gaseous pollutants in situ. The number of pilot projects is however growing

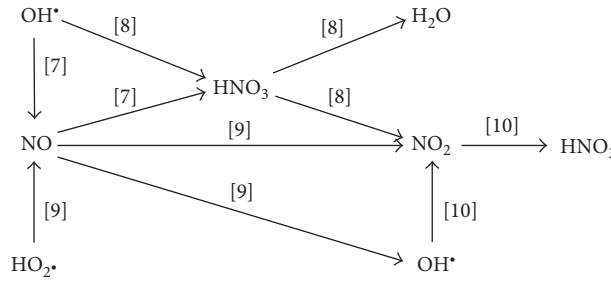

Figure 2: Photocatalytic oxidation of NO over TiO_2.

since recent years, and literature reports more and more field campaigns conducted in urban environments for air purification purposes [29–35, 37–39].

Another important point when dealing with air depollution by photocatalysis is the illumination conditions. In order to initiate the degradation process, pure TiO_2 requires photoexcitation with light at wavelengths matching the band gap of the active anatase phase (3.2 eV), that is, wavelengths shorter than 388 nm. This wavelength range is unfortunately scarce in indoor environments in which the ability of the TiO_2 photocatalyst to degrade gaseous pollutants appears to be limited. Several methods employed to make TiO_2 photocatalyst active under visible light are reported in the literature. One route is by doping pure TiO_2 with foreign atoms [18, 40]. For example, transition metals such as cobalt (Co), copper (Cu), and iron (Fe) narrow the band gap of TiO_2 and cause a redshift of the absorption edge to the visible-light region [41–43]. TiO_2 can also be doped with nonmetal elements such as carbon (C), nitrogen (N), or fluorine (F) [44, 45].

In this paper, NO was photocatalytically oxidized over titanium dioxide semiconductor using functional coatings intended to improve indoor air quality. Focus was made here on three experimental parameters which are of great importance in making photocatalysis efficient and successful: the amount of TiO_2 particles available at the surface, the nature of the substrate, and the illumination conditions. Mortar and wood substrates were coated with TiO_2 dispersions at various concentrations. Therefore, from high to low TiO_2 dry matter contents on the surface were obtained. Wood is worth studying as its use as an indoor building material is

(a) (b) (c)

Figure 3: Surface appearance of substrates tested: mortar W/C = 0.4 (a), mortar W/C = 0.5 (b), and painted wood (c). Surface roughness mean values: 130 μm, 11 μm, and 15 μm for mortar W/C = 0.4, mortar W/C = 0.5, and wood (see Section 3.2).

becoming more and more common. A series of experiments was conducted at laboratory scale based on the setup and procedure described in the ISO standard [25]. The influence of the illumination conditions was explored using artificial light: UV light and visible light. The visible fluorescent tube used here produced a short-wave ultraviolet light, which may be sufficient to initiate photocatalysis. NO and NO_2 concentrations were measured with a NO_x analyser. By comparing the NO inlet and outlet concentrations, NO abatements were evaluated for all the experiments conducted and the influence of the TiO_2 dry matter content on the surface, the nature of the substrate, and the light was assessed.

2. Materials and Methods

2.1. TiO_2 Dispersions. Photocatalytic dispersions tested here were prepared from CristalACTiV™ S5-300B. This commercial product is a stable aqueous dispersion of ultrafine TiO_2 anatase particles with a specific surface of 330 m^2/g. TiO_2 dry matter content in CristalACTiV S5-300B is 18 wt%. This value was confirmed by drying in a 100°C oven for 24 hours. Various TiO_2 aqueous dispersions were obtained by dilution of CristalACTiV S5-300B in water. After mixing, the TiO_2 dispersions were applied to the substrates before the settling occurred. The concentration range tested was broad, from high to low TiO_2 dry matter content in solution: 18 wt%, 12 wt%, 6 wt%, 4 wt%, and 1 wt% for all the substrates. Two additional concentrations were tested for mortars: 5 wt% and 3 wt%. As it will be discussed further on, surfaces having a TiO_2 dry matter content as low as 2 g/m^2 after treatment with a CristalACTiV S5-300B dispersion showed significant abatement values depending on the substrates and lighting conditions.

2.2. Substrates. Common building materials have been explored in this paper: mortar and wood. In order to obtain different roughness, two formulations of mortar were tested: mortar with a water-cement ratio of 0.4 (W/C = 0.4, higher roughness) and normalized mortar with a water-cement ratio of 0.5 (W/C = 0.5, lower roughness). The formulation and preparation of the mortars were adapted from the NF EN 196-1 standard [46]. They were made with siliceous sand (granulometry: 0/2 mm) and CEM I 52.5 Portland cement. Mortar preparation was carried out at ambient temperature and relative humidity of 55%. Each sample (mortar W/C = 0.4 and mortar W/C = 0.5) was mechanically mixed according to [46] standard during 3.5 min and then cast in a $300 \times 300 \times 10\,mm^3$ steel mould with the aid of a vibrating table. The resulting slab was kept covered in a room at constant temperature and humidity. It was finally demolded after 5 days and then sawn into $100 \times 50 \times 10\,mm^3$ samples on which TiO_2 coating was applied. For wood sample, commercial painted spruce panel (Protect Ouest-LAMEXEL) was used and sawn into $100 \times 50 \times 10\,mm^3$ before being coated with TiO_2 dispersion. Mortar and wood samples, referred as control samples, were preserved from any coating.

The objective of testing various substrates was to assess the effect of surface roughness on photocatalytic efficiency. Mortar is a porous material representative of concrete blocks, concrete wall, and mortar coatings and is the object of most of the studies dealing with air depollution and self-cleaning by photocatalysis. Unlike, the behavior of wood under photocatalytic activity is still unknown. The substrates tested are shown in Figure 3.

2.3. Coating Method. Photocatalytic activity is greatly influenced by the technique used for depositing the photocatalytic material and by the substrate nature. As photocatalysis is a surface phenomenon and direct interaction of TiO_2 with UV illumination is essential, mixing TiO_2 into traditional mortar or concrete can only have limited NO degradation effect at the air/solid interface. In this case, the amount of TiO_2 used is high, and most of the photocatalyst is wasted in the internal structure where light is not available [47]. The coating technique appears to be more beneficial as an ultra-thin film that exposes the nanosized TiO_2 particles to the polluted atmosphere can be formed at the surface. It results in lower TiO_2 consumption and leads to cost reduction. Moreover, TiO_2 dispersions can be applied to existing structures following various application methods and used for any kinds of building materials [20, 48–50]. However, further progress is needed as TiO_2 coatings may show a reduction in their efficiency (due to abrasion) after few months of use [51]. In this study, the TiO_2 dispersion was applied to the substrate surface using a fine brush. The amount of TiO_2 deposit on the surface was controlled and determined by weighing the recipient containing the TiO_2 dispersion and the brush before and after coating the sample. A first TiO_2 deposit on the surface was completed followed by a drying step for 1 hour at ambient temperature and humidity. A second deposit was then realized, and the samples were again allowed to dry before experiments were conducted in the reactor. It has to be noted that the same surface treatment protocol was followed for all the substrates tested.

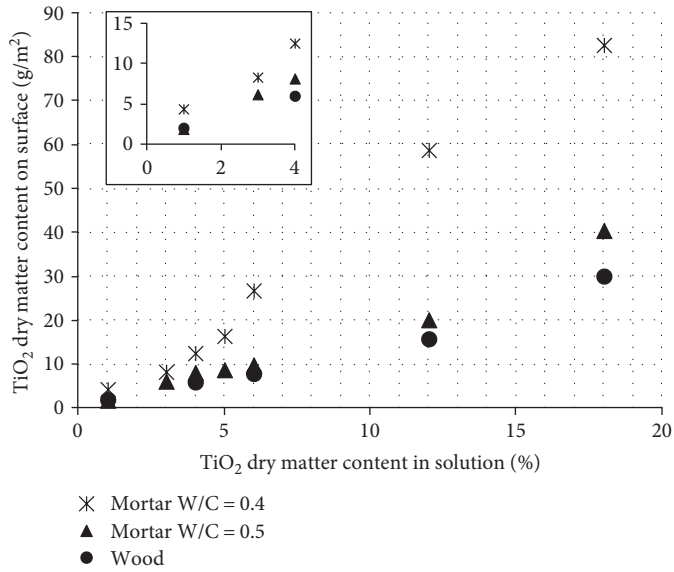

Figure 4: Correlation between TiO_2 dry matter content in solution (%) and TiO_2 dry matter content on the surface (g/m^2). The dry matter content of TiO_2 on the surface was obtained by dividing the total TiO_2 deposit by the surface of the sample and multiplying by the percentage of TiO_2 in solution. Each point is the mean value of three samples (cf. Figure 5).

Each photocatalytic dispersion with a specific TiO_2 dry matter content (18 wt%, 12 wt%, 6 wt%, 5 wt%, 4 wt%, 3 wt%, and 1 wt%) was applied to the mortar and wood samples. As a matter of fact, because of different roughness, it was expected that for the same TiO_2 dispersion, the TiO_2 deposit changed between the substrates resulting in different TiO_2 dry matter content available at the surface. Figure 4 shows the correlation between TiO_2 dry matter content in solution expressed in percentage and TiO_2 dry matter content on the surface expressed in g/m^2. The dry matter content of TiO_2 on the surface was obtained by dividing the total TiO_2 deposit by the apparent surface of the sample and multiplying by the percentage of TiO_2 in solution. Each point in Figure 4 represents the mean value of TiO_2 dry matter contents obtained from three samples. We clearly observe the different behaviour between the three substrates with W/C = 0.4 mortar allowing the higher amount of TiO_2 to be applied to the surface. The rougher surface of this mortar could be a reasonable explanation with a higher developed surface area leading to an increase in the bonding between substrate and TiO_2 particles. The surface appearance of the tested two mortars and wood samples can be seen in Figure 3, and an estimation of their roughness is presented below in Section 3.2.

Figure 5 presents the TiO_2 dry matter content expressed in g/m^2 obtained on the surface for the three substrates tested when using the 12 wt% TiO_2 dispersion. These results show that the coating method used here was repeatable for each kind of substrate. In the following statement, the TiO_2 dry matter content expressed in g/m^2 will be used as it is representative of the amount of TiO_2 directly available on the surface which can potentially degrade NO.

2.4. Experimental Setup. A laboratory environmental setup was used to evaluate the NO removal efficiency due to TiO_2 photocatalytic effect. It was placed in an air-conditioned room at 20°C. The experimental setup is shown in Figure 6. An air generator (Environnement S.A., France, model ZAG7001) supplied two ultra-pure dry air (or zero-air) streams by filtering ambient air. The flow rate of each purified air streams was adjusted by a mass flow controller (Bronkhorst). One purified air stream was humidified by passing through a gas washing bottle. By varying the flow rate of this stream, the desired humidity level can be obtained. The total air stream was then mixed with NO stream which was also adjusted using a mass flow controller (Bronkhorst). NO coming from a compressed gas cylinder (Air Liquide, France) with an initial concentration of 8 ppm was balanced with

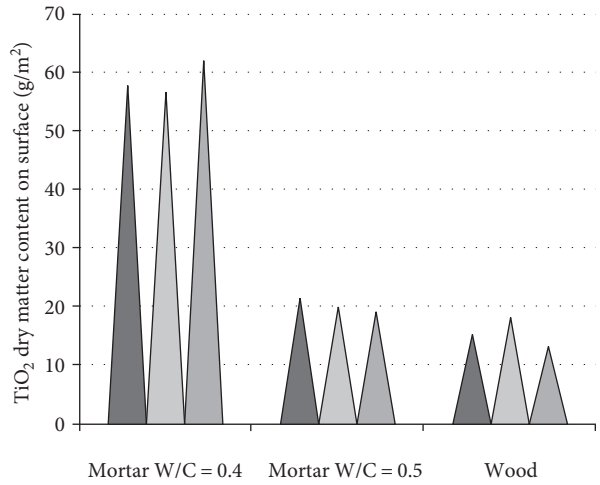

Figure 5: TiO_2 dry matter content in g/m^2 obtained on the surface for the three substrates tested when using the 12 wt% TiO_2 dispersion. The coating method was used for each substrate sample.

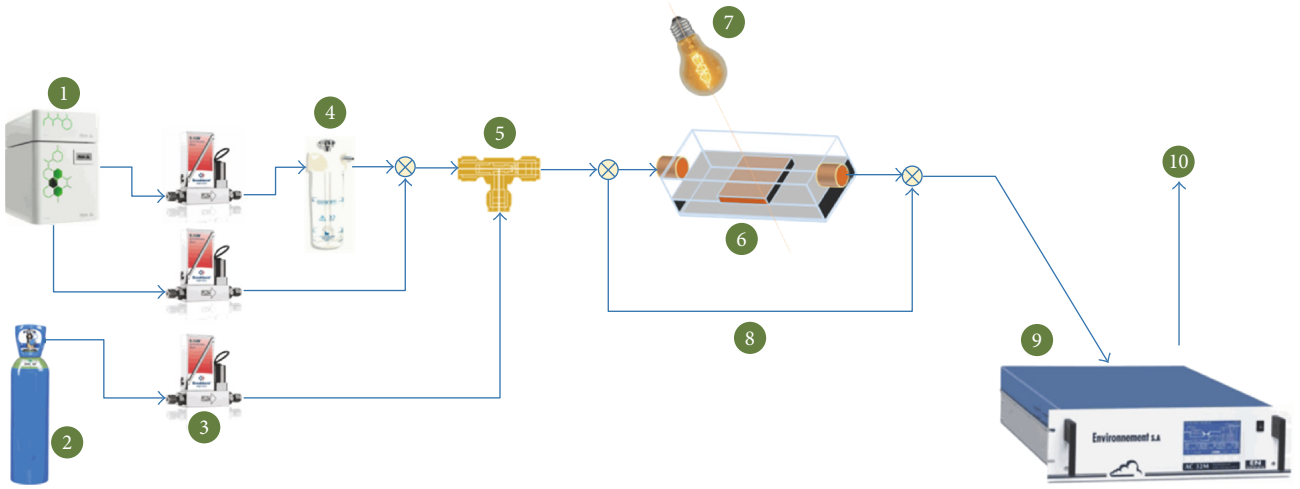

Figure 6: Schematic diagram of the experimental apparatus for NO degradation: (1) zero-air generator; (2) NO gas cylinder (8 ppm); (3) mass flow controllers; (4) gas washing bottle; (5) mixing chamber; (6) borosilicate-glass reactor with temperature and relative humidity probes; (7) lighting system; (8) bypass; (9) NO_x analyser; and (10) an extraction system.

Table 1: Illumination conditions tested.

	Reactor-tube distance	UV-A region (315–400 nm)	VIS region (400–800 nm)
OSRAM Lumilux Cool White T8	45 cm	0.035 W/m^2	2.4 W/m^2
NARVA Blacklight Blue T8	45 cm	1.0 W/m^2	Negligible
	15 cm	3.3 W/m^2	Negligible

nitrogen and diluted to 400 ppb for all the experiments. The polluted air then flowed continuously through the reactor, and the NO_x concentration was measured each 5 s step at the reactor exit using a NO_x chemiluminescent analyser (Environnement S.A., France, model AC3 2 M). This analyser displayed NO_x, NO, and NO_2 concentrations; NO_2 concentrations are being calculated from the difference between NO_x and NO concentrations. However, it has recently been observed that this kind of analyser could overestimate the NO_2 concentration as it seemed to measure all NO_y entering in the NO_x channel [24, 52].

A borosilicate-glass reactor with a cylindrical shape (diameter = 60 mm, length = 300 mm) equipped with a PTFE sample holder was used for its low adsorption capacity and its high transparency to UV-A [20]. Control and coated samples ($100 \times 50 \times 10$ mm^3) were placed on the sample holder in the median plane of the reactor resulting in a gas circulation through the semicylindrical space between the sample and the upper part of the reactor (free volume of 424 cm^3). The temperature and the relative humidity inside the reactor were monitored over time using a probe. This photocatalytic reactor creates an enclosed controlled environment in which a polluted atmosphere is simulated.

2.5. Illumination Conditions. The illumination conditions were controlled using fluorescent tubes placed above the photocatalytic reactor. They are summarized in Table 1. It can be seen that the chosen visible fluorescent tube had a broad wavelength range and slightly produced light in the UV-A region. Depending on the light type and the distance between the source and the upper surface of the reactor, three different illumination conditions were tested: UV light at 1 W/m^2, UV light at 3.3 W/m^2, and VIS (visible) light at 2.4 W/m^2. The light intensity was measured using a radiometer (Gigahertz-Optik) equipped with two detectors: UV-A radiometric detector (UV-3717 model, $315 < \lambda < 400$ nm) and VIS detector (RW-3703 model, $400 < \lambda < 800$ nm). UV light was obtained by using a blacklight blue fluorescent tube of 18 W emitting in the UV-A region of the spectrum UV (NARVA Blacklight Blue T8 18 W-073, dominant wavelength: 370 nm). The two different light intensity values were obtained by varying the position of the fluorescent tube, that is, the distance between the upper surface of the reactor and the tube. Placing the tube near the reactor, that is, at a low position (15 cm), allowed having a UV light intensity of 3.3 W/m^2 on the reactor's upper surface. On the contrary, increasing the distance between the reactor and the fluorescent tube, thus placing the tube at a higher position (45 cm), resulted in a lower UV light intensity value of 1 W/m^2. Visible light was obtained by using a fluorescent tube of 18 W (OSRAM Lumilux Cool White T8 18W-840). Intensity values of 2.4 W/m^2 and 0.035 W/m^2 were, respectively, measured with the VIS detector and UV-A detector when placing the VIS light tube at a high position (45 cm). It has to be noted that the test procedure described in ISO 22197-1 [25] requires a light intensity of 10 W/m^2 in the UV-A region.

A monitoring campaign on UV light intensity was conducted in three different rooms in INSA-LMDC building located in Toulouse, south of France: a laboratory room R1

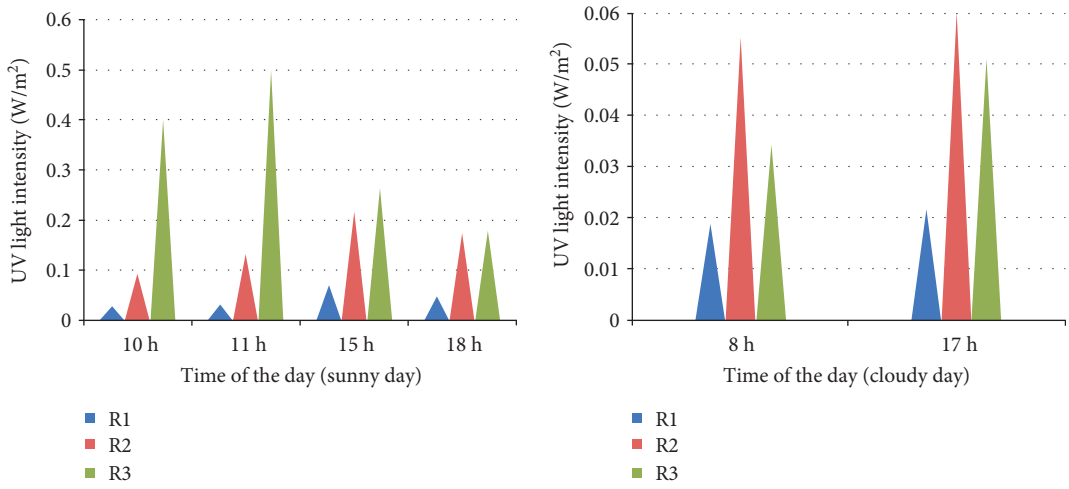

Figure 7: UV light intensity available during daytime in three rooms (not under direct sunlight): a laboratory room (R1) and two classrooms (R2 and R3) on sunny and cloudy days in April in Toulouse, south of France (beware of the *y*-axis scale on the graphs).

which had a 2 m^2 sky window and two classrooms R2 and R3 with, respectively, a window surface of 8.5 m^2 in the South-West and a window surface of 16.8 m^2 in the South-East. The measurements were made on sunny and cloudy days in April at different hours by using the radiometer and the UV-A detector. The following procedure was followed: the artificial light in the room was first switched on for 5 min, the UV-A detector was then placed in the centre of the room on a table (avoiding direct sunlight), and the UV-A intensity value was finally measured with the radiometer. The rooms were chosen according to their location and the number of windows through which natural light could enter. The aim of these measurements was not to precisely analyze the natural indoor light conditions but rather to identify the UV light intensity available during daytime in real-world conditions and compare it with the irradiance applied to the borosilicate-glass reactor to activate TiO_2. The values are presented in Figure 7.

These results show that the UV light intensity may vary during daytime depending on the localization and brightness of the room. Indoor UV light intensities ranged between 0.02 and 0.50 W/m^2 with the lowest values being observed on a cloudy day for the laboratory room which had only a sky light as window. One has to note that the proportion of UV for the VIS light condition tested at the laboratory scale was 0.035 W/m^2. This UV intensity could thus be obtained in real-world conditions providing the window surface was high enough (cf. rooms R2 and R3).

2.6. Experimental Protocol. The experimental procedure used in this study was inspired by ISO 22197-1 [25]. It enabled to determine the ability of a photocatalytically active material to degrade NO by supplying a polluted air continuously throughout the reactor, while providing UV or VIS light to activate the photocatalyst. The first step of this experimental procedure was carried out in the dark. NO gas pollutant was diluted to 400 ppb using a mix of dried and humidified air streams tuned by mass flow controllers. Firstly, in order to control and adjust the NO inlet concentration to the target value (i.e., 400 ppb), the polluted air went through the bypass (cf. Figure 6) directly to the analyser. Its flow rate was maintained constant at 1.5 L/min and flow rates of NO gas and dried and humidified air streams were eventually adjusted to get 400 ppb of NO. Once the NO concentration displayed by the analyser was stable, polluted air was allowed to flow through the upper part of the cylindrical reactor for 15 min. Under the conditions tested here, the gas flow was laminar ($R_e \approx 50$). As seen in Figure 8, a decrease in NO concentration was immediately observed due to the filling time of the reactor and NO adsorption on the surface of the sample and the exposed surface area of the reactor. Once NO concentration returned to its initial value, light was switched on to initiate photocatalytic reactions: an instantaneous decrease in NO concentration was observed. This second step of the experimental procedure conducted under illumination lasted 60 min. The NO concentration remained mostly constant throughout this period. The light was then switched off again, and the NO and NO_x concentrations were measured in the dark for 15 min before stopping the experiment. Figure 8 shows the typical evolution of NO, NO_2, and NO_x concentrations during a test conducted on mortar W/C = 0.4 under UV light at 1 W/m^2 with a TiO_2 dry matter content on surface of 8 g/m^2. A decrease in NO concentration was clearly observed once the light was switched on. However, its degradation led to the generation of NO_2 according to reactions 8 and 9 (cf. Figure 2).

The photocatalytic performance of the various samples coated with TiO_2 dispersion was assessed by two degradation ratios calculated as follows:

$$\mathrm{NO}^{\mathrm{deg}}(\%) = 100 \times \frac{[\mathrm{NO}]_{\mathrm{in}} - [\mathrm{NO}]_{\mathrm{out}}}{[\mathrm{NO_x}]_{\mathrm{in}}} > 0,$$
$$\mathrm{NO_2}^{\mathrm{deg}}(\%) = 100 \times \frac{[\mathrm{NO_2}]_{\mathrm{in}} - [\mathrm{NO_2}]_{\mathrm{out}}}{[\mathrm{NO_x}]_{\mathrm{out}}} < 0, \quad (1)$$

where $[NO]_{in}$, $[NO_2]_{in}$, and $[NO_x]_{in}$ are the inlet concentrations in the dark once the stable regime was established;

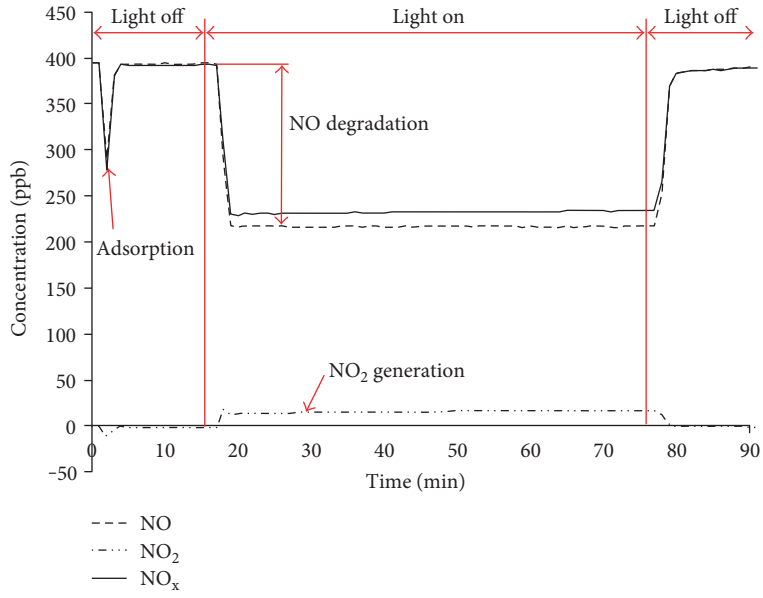

Figure 8: Typical evolution of NO, NO_2, and NO_x (i.e., $NO + NO_2$) concentrations during a test conducted on mortar W/C = 0.4 under UV light at 1 W/m^2 with a TiO_2 dry matter content on surface of 8 g/m^2.

$[NO]_{out}$, $[NO_2]_{out}$, and $[NO_x]_{out}$ are the average outlet concentrations measured during the 60 min illumination period. A negative degradation ratio means that intermediate products are formed, which is the case for NO_2^{deg} (%). Unlike, a positive value reveals a decrease in the pollutant concentration, which is the case for NO^{deg} (%).

The temperature and relative humidity measured inside the reactor with the probe for all the realised experiments varied, respectively, between 21 and 24°C and 25 and 43% (instantaneous values) because of the illumination by the lamp and the slight variations in ambient air conditions. However, for a single experiment, temperature and humidity were stable ($\Delta T = \pm 0.5$°C and $\Delta HR = \pm 1\%$). In this range of temperature, the humidity varied between 4 g/kg and 8 g/kg. As previously reported in [20], no significant influence of humidity on NO degradation ratio was observed for an NO initial concentration of 400 ppb and 1000 ppb (the humidity range tested in [20] was 0–14.5 g/kg at 25°C). A significant decrease in the degradation ratio was however noted for higher concentrations (1500 ppb and 2000 ppb) at humidity level lower than 4 g/kg for mortar substrates and 6 g/kg for glass substrates. In our experimental conditions (temperature and humidity ranges, NO concentration, flow reactor, flow rate, and light intensity), the degradation ratios were found to be independent of humidity.

The experimental procedure described above was used to test the influence of three parameters on the photocatalytic efficiency to degrade NO, namely, TiO_2 dry matter content applied to the surface, illumination conditions, and substrate nature. For each substrate, experiments on control samples (i.e., samples not coated with TiO_2 dispersion) were also carried out in order to investigate a possible photolysis (i.e., the degradation of NO caused directly by the light) and adsorption phenomenon. The obtained results proved that within the limits of experimental error no significant reduction of NO concentration by photolysis or adsorption occurred for the control substrates tested in this study.

3. Results and Analyses

3.1. Influence of TiO_2 Dry Matter Content on Photocatalysis Efficiency. The TiO_2 aqueous dispersions were prepared as described in Section 2.1 and applied to substrates following the coating method presented above. Degradation ratios obtained for each substrate and for different dry matter contents of TiO_2 applied to surfaces (expressed in g/m^2) are shown in Figures 9(a), 9(b), and 9(c) (mortar W/C = 0.4, mortar W/C = 0.5, and wood, resp.). The positive degradation ratios are associated to a decrease in NO concentrations due to photocatalytic activity occurring during the illumination period. The negative values are associated to the generation of NO_2 due to the oxidation of NO to NO_2 during the photocatalysis. The results obtained for the three substrates under three different illumination conditions are also represented in Figure 9 but will be discussed in the following parts. Focus is mainly made here on the effect of TiO_2 dry matter content on photocatalysis efficiency as it is a relevant parameter for the degradation process. For example, in [53], authors showed that TiO_2 product related parameters, such as application technique, TiO_2 type, and powder content, were of great influence. The degradation ratio of photocatalytic concretes was improved with increasing TiO_2 powder content in the bulk. Unlike, Shen et al. [50] observed that in the case of a coating treatment method, the NO degradation ratios for different TiO_2 concentrations were similar. The tested coating technique was still effective with a small amount of TiO_2, which resulted in material cost savings.

For the mortar with the lowest water-cement ratio (W/C = 0.4), the TiO_2 dry matter content seems to have

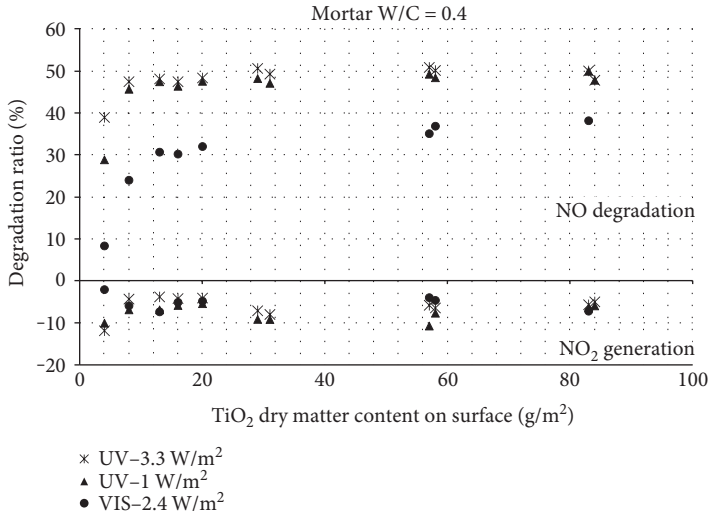

(a)

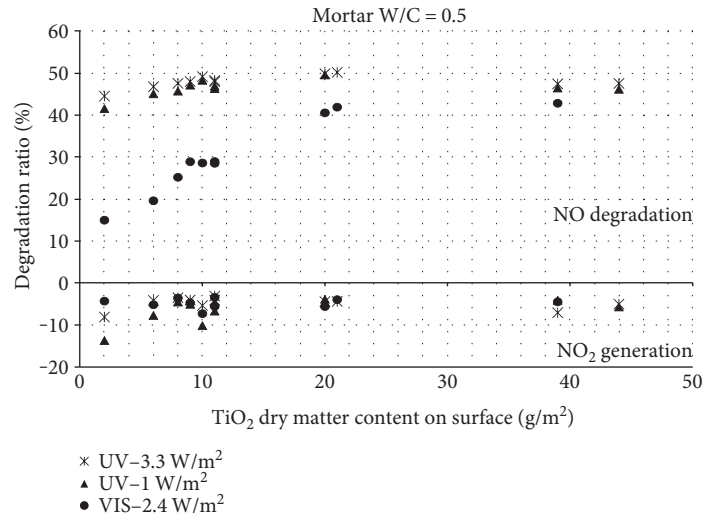

(b)

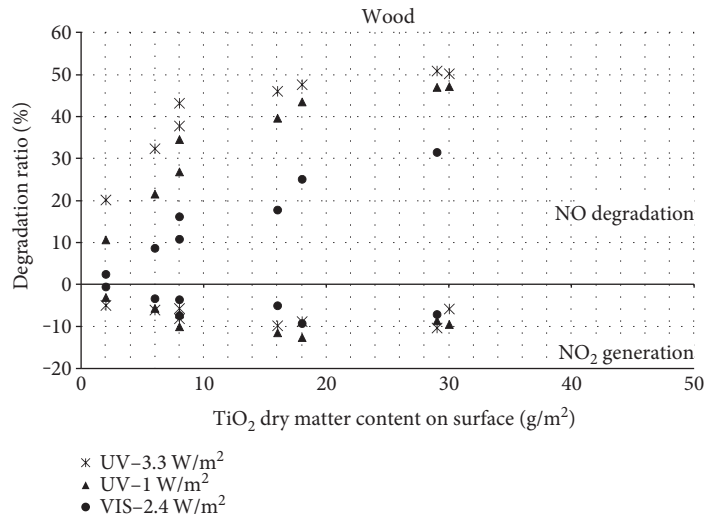

(c)

Figure 9: Influence of TiO_2 dry matter content applied to surface (in g/m^2) on NO degradation ratio (in %) for each substrate under three different illumination conditions (the NO_2 generation is also represented): (a) mortar W/C = 0.4, (b) mortar W/C = 0.5, and (c) wood.

no significant effect under UV light for values higher than 8 g/m^2. NO degradation ratio ranges from 46 to 50% which means that in these conditions the photocatalysis is clearly efficient. Moreover, these results suggest that there is an optimal TiO_2 dry matter content (i.e., 8 g/m^2) above which the degradation ratio does not increase significantly and tends to approach a constant value. For high dry matter content, the layer of TiO_2 on surface becomes too thick and a proportion of the photocatalytic product is inefficient due to the absence of direct interaction with UV illumination and contact with pollutants. The optimal TiO_2 content corresponds to the maximum photocatalytic surface area accessible to pollutants and light to promote reduction-oxidation reactions. The same trend is observed under VIS light but with a higher optimal TiO_2 dry matter content: around 20 g/m^2 instead of 8 g/m^2 for UV light. In the case of mortar with W/C = 0.5, a quite similar behavior may be observed: the NO removal efficiency reaches a maximum from 8 g/m^2 and 20 g/m^2 under UV light and VIS light, respectively. For TiO_2 surface coating lower than 8 g/m^2, the photocatalysis is slightly less efficient with NO degradation ratios varying from 8.5 to 39% for mortar W/C = 0.4 with TiO_2 surface coating of 4 g/m^2 and from 15 to 44.5% for mortar W/C = 0.5 with TiO_2 surface coating of 2 g/m^2 depending on the illumination conditions.

For wood substrate, no plateau appears for the NO degradation ratio. For TiO_2 dry matter content varying from 2 to 30 g/m^2, the NO degradation ratio increases whatever the illumination conditions are and even reaches 50% under UV light, which is the value obtained for mortar samples. It has to be noted that a further increase in degradation ratio for wood sample could be observed for TiO_2 dry matter content higher than 30 g/m^2. For TiO_2 surface coating of 2 g/m^2, NO degradation ratios are quite low compared to mortar samples: a variation from 2.5 to 20% is observed depending on the illumination conditions.

Figure 9 shows negative degradation ratios corresponding to the generation of NO_2. At a laboratory scale, when NO is degraded by photocatalysis, NO_2 is produced over titanium dioxide as a by-product. Here, values between −3 and −13.5% were obtained for all the samples tested. This small variation range makes it difficult for the analysis of the NO_2 results and the correlation between NO_2 generation and the parameters studied (i.e., TiO_2 dry matter content applied to the surface, illumination conditions, and substrate nature). However, two trends can be noted. Firstly, NO_2 generation seems to slightly increase with TiO_2 dry matter content for the wood sample. Secondly, NO_2 generation seems to be twice higher on wood than on mortar for the same quantity of TiO_2 (around 18–20 g/m^2).

As reported in the literature [15, 16], the photocatalytic degradation of NO occurs in two stages according to reactions 7 to 10 presented in Figure 2: first, oxidation of NO to NO_2 and then, oxidation of NO_2 to nitrate ions NO_3^-. The measured NO_2 concentration could be the consequence of the competition for adsorptive sites between NO and NO_2 on the one hand and between NO_2 and NO_3^- on the other hand [20]. Moreover, the lower kinetics of reaction 10 could also promote the increased presence of NO_2. Modifying TiO_2 nanoparticles could be a way to prevent NO_2 generation. Recently, Karapati et al. [54] modified TiO_2 P25 nanoparticles with silane coupling agent. They showed that the modified powder obtained increased hydrophilicity and thus promoted NO degradation but also diminished NO_2 formation. The resulting product was found to possess high De-NO_x ability (NO degradation was enhanced 2–5 times in comparison with commercial P25). In addition, in [55], Karapati et al. modified P25 with hydrophilic polyethylene glycol and hydrophobic oleylamine, a mixture of both and compared the De-NO_x efficiency. They showed that all three modified TiO_2 nanoparticles exhibited higher NO_x removal (higher NO degradation and lower NO_2 generation) than standard P25. According to these authors, modifying surface hydrophilicity diminished NO_2 production because the deficiency of hydroxyl radicals promoted the oxidation of NO_2 to NO_3^-.

Furthermore, substrate nature plays a significant role in the detection of NO_2 generated. It is known that NO_2 is adsorbed on substrate surface [56]. Since mortar is a porous material, the observed difference of NO_2 production in our results may be due to adsorption. In addition, alkali compounds of mortar (portlandite) can contribute to NO_2 adsorption [57]. Using clay substrates made from minerals like talc and hydrotalcite can also enhance the De-NO_x efficiency of photocatalysis [58]. Like mortar, these substrates have an alkali character: not only NO_2 adsorption is promoted but also NO is directly transformed to NO_3^-, that is, without generating NO_2.

3.2. Influence of Substrate Nature on Photocatalysis Efficiency. NO degradation ratios obtained for two TiO_2 dry matter contents (i.e., 8 g/m^2 and 18–20 g/m^2) applied to the surface of each substrate (mortar W/C = 0.4, mortar W/C = 0.5 and wood) are shown in Figure 10 by using histogram graphs.

These results highlight the influence of the substrate nature on NO removal efficiency by photocatalysis. For the same TiO_2 dry matter content on surface, mortar samples show the best degradation ratios. Between the two mortars tested here, no difference is observed for a TiO_2 dry matter content of 8 g/m^2. However, for higher concentration of TiO_2 applied to surface (i.e., 20 g/m^2), mortar with a water-cement ratio of 0.5 shows a slightly better photocatalysis efficiency. The same is true for lower TiO_2 surface-coating values such as those tested here: 2 g/m^2 for mortar W/C = 0.5 and 4 g/m^2 for mortar W/C = 0.4. Mortar W/C = 0.5 has indeed a NO degradation ratio almost two times higher than mortar W/C = 0.4 although two times less photocatalytic product was applied to its surface (cf. Figure 9). As previously explained in Section 2.3, W/C = 0.4 mortar substrate was the one allowing the higher amount of TiO_2 to be deposited on the surface probably because of its rougher surface. Hassan et al. [49] realized laboratory weathering tests on substrate concrete samples coated with TiO_2 using a loaded-wheel tester. NO removal efficiency was observed after weathering action for concretes on which a water-based TiO_2 surface treatment was applied. The authors suggested that the exposed part of the embedded TiO_2 particles at the surface was increased for weathered concrete samples.

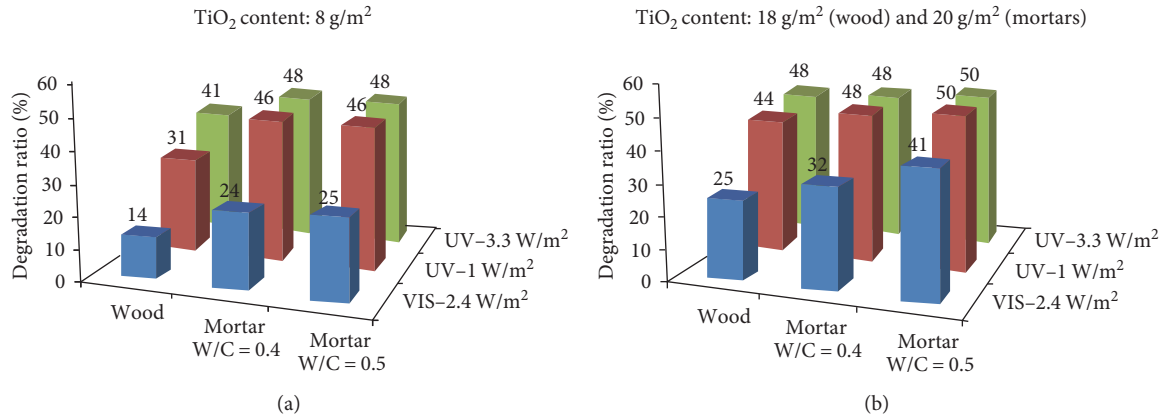

FIGURE 10: Influence of substrate nature on NO degradation ratio (in %) for two TiO_2 dry matter contents applied to the surface (in g/m^2) of each substrate under three different illumination conditions: (a) 8 g/m^2 applied to all substrates, (b) 18 g/m^2 applied to wood, and 20 g/m^2 applied to mortars. The accuracy of the measurements is ±0.5%.

Moreover, in [59], authors showed that high porosity and roughness values favored the retention of TiO_2 particles on the substrate surface after dip-coating on cementitious materials and were critical parameters to obtain efficient photocatalytic properties to purify air from airborne VOC. However, in the experiments conducted here, as TiO_2 was applied to surfaces using a brush, roughness seems to be a more adequate parameter rather than porosity to compare the efficiency of mortars to degrade NO. In the case of rougher surfaces, direct interactions between TiO_2 particles and light may decrease because of shadow effects due to the relief and because of the random orientation of the surface facets. Some TiO_2 particles are thus less accessible to light which results in a limited NO reduction effectiveness. Moreover, as highlighted in [60], the results presented here may raise the question of the importance of the exposed surface area when dealing with photocatalysis. Limiting the amount of photocatalytic product applied to the surface as well as the roughness of the substrate seems to be of utmost interest to obtain the highest exposed surface area and thus the optimal photocatalysis efficiency.

To go further in the roughness characterization, a first surface measurements campaign with a confocal laser scanning microscope (Olympus LEXT OLS3100) was carried out on each substrate. This technique involves sequentially illuminating the focal plane with a diffraction-limited light spot point by point. Specimen information is transmitted back through the optics via a confocal aperture which rejects light out of the focal plane. It sequentially scans through the specimen field of view which enables a 2D digital image of the focal plane to be formed thanks to a photomultiplier tube which transforms the light signal into an electrical one. By collecting a series of adjacent 2D digital images captured at different depths, 3D images can be constructed and roughness values can be deduced. A 1×1.2 mm^2 surface was analyzed for the three substrates. The measuring step according to z-axis was set to 2 μm for the mortar W/C = 0.4 control sample and to 1 μm for the mortar W/C = 0.5 and wood control samples. After obtaining the first 3D images, values were filtered using a Gaussian approximation algorithm in order to eliminate the background noise (cf. Figure 11(c)). Image processing was then carried out using a smoothing function to remove peaks and singularities and obtain clearer and softener 3D images (cf. Figures 11(a) and 11(b)). The surface roughness was deduced from the average height variation for different plane sections in the x- and y-axes. Obtained mean values were, respectively, 130 μm, 11 μm, and 15 μm for mortar W/C = 0.4, mortar W/C = 0.5, and wood. A clear difference is observed between the substrates, which is coherent with the correlation between TiO_2 dry matter content in solution and TiO_2 dry matter content on the surface observed in Figure 4. Indeed, according to Figure 4, mortar W/C = 0.4 shows the highest ability to keep TiO_2 particles on its surface and in the same time proves to be the rougher surface from confocal laser scanning microscope measurements. On the contrary, mortar W/C = 0.5 and wood show a ten times lower roughness which could hinder the retention of TiO_2 on their surface. It should be mentioned that further work has to be done on roughness measurements with this technique to confirm these results and the influence of other parameters (such as pH of substrate, light absorption) has to be investigated. However, as explained above, a higher surface contact between TiO_2 particles and NO molecules due to a higher roughness does not necessary favor the photochemical oxidation because of the limiting access to light.

3.3. Influence of Illumination Conditions on Photocatalysis Efficiency. The influence of the illumination conditions can be observed in Figures 9 and 10 and are dependant of the nature of substrate. It can be noted that the higher NO degradation ratios are obtained under UV illumination whatever the substrate: abatement values around 50% are reached for the three substrates. For mortar samples, NO removal efficiency is quite similar under the two UV light intensities tested (1 W/m^2 and 3.3 W/m^2), with values under 3.3 W/m^2 UV illumination being slightly higher. As previously explained, the TiO_2 dry mortar content has no significant influence in these conditions. However, for the wood sample, the difference in degradation ratio is much more pronounced

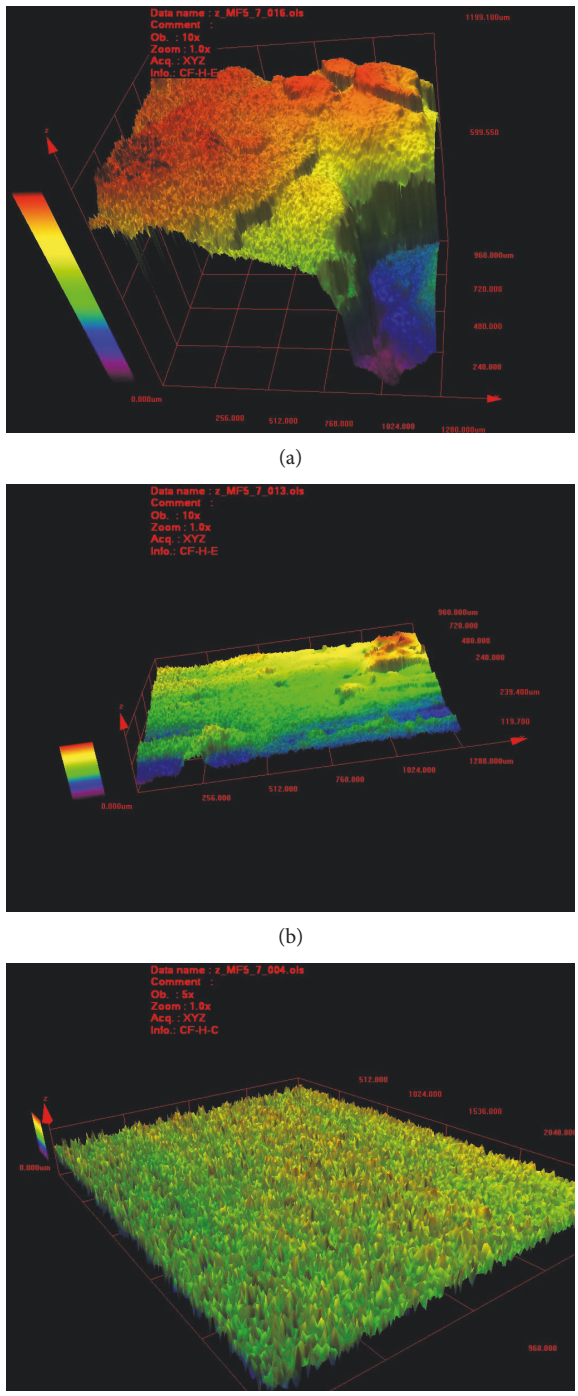

(a)

(b)

(c)

FIGURE 11: 3D images ($0 < x < 1280\ \mu$m; $0 < y < 960\ \mu$m; z variable) obtained from surface samples analyzed with confocal laser scanning microscope: (a) mortar W/C = 0.4, 600 steps of 2 μm with an optical zoom x10, (b) mortar W/C = 0.5, 250 steps of 1 μm with an optical zoom x10, and (c) wood, 200 steps of 1 μm with an optical zoom x5.

between the two UV light intensities, with values being between 6 and 29% lower under 1 W/m^2 UV illumination. This deviation becomes however narrower when the TiO_2 dry matter content applied to wood surface increases.

Experiments conducted under VIS light show lower NO degradation ratios. The maximum values reach 32%, 38%, and 43% for wood, mortar W/C = 0.4, and mortar W/C = 0.5 samples, respectively. However, the proportion of UV in the VIS light being relatively low, around 0.035 W/m^2 as measured by the radiometer, these abatement values can be considered as quite efficient and bright for photocatalytic oxidation technology in indoor conditions. In spite of the generated data, such results have not been reported in the literature, yet they have been confirmed by a series of experiments. The UV light intensity monitoring campaign presented in Section 2.5 has shown that a UV light intensity as low as 0.019 W/m^2 was obtained in an indoor environment on cloudy days meaning that similar degradation ratios could be obtained in real-world conditions where NO_x concentrations are lower. Moreover, by choosing adequate visible lamps, such as fluorescent tubes, indoor natural UV light intensity may be artificially increased resulting in a better activation of photocatalysis and NO degradation.

4. Conclusion

In this paper, the influence of three parameters on NO photocatalytic degradation was assessed: TiO_2 dry matter content, nature of the substrate, and light conditions. Three different substrates were used—mortar W/C = 0.4, mortar W/C = 0.5, and painted wood—on which various TiO_2 dry matter contents were applied by means of a coating treatment. These samples were subjected to NO dynamic injection in a standardized reactor under three different illumination conditions: UV light at 3.3 W/m^2, UV light at 1 W/m^2, and VIS light at 2.4 W/m^2. According to the authors, the main novelties are the used of wood as substrate, the low TiO_2 dry matter content applied to surfaces, and the low UV light intensity to simulate the indoor environment.

The results showed that the substrate nature greatly influenced the bonding between TiO_2 particles and the substrate with rougher surface allowing higher amount of TiO_2 to be applied. However, the best photocatalytic activity was obtained with substrate having a moderate roughness and a limited TiO_2 content on surface. NO degradation ratios reached indeed an optimal value for mortar substrates meaning that higher TiO_2 deposit on the surface did not improve the photocatalysis anymore. A too thick TiO_2 layer at the sample surface was indeed inefficient due to the absence of direct interaction between TiO_2 particles, pollutants, and light promoting reduction-oxidation reactions. Moreover, in the case of a too rough surface as it was observed for mortar W/C = 0.4, some particles were indeed less accessible to light which could result in a decrease in NO degradation ratio. Limiting the amount of functional photocatalytic coating applied to the surface as well as the roughness seems to be primordial to obtain the best-exposed surface area and thus the optimal photocatalysis efficiency. Concerning the influence of light conditions, the experiments conducted under UV illumination showed the highest photocatalytic performance whatever the substrate nature: NO degradation ratios as high as 50% could be obtained. UV-A light is indeed the

most suitable range regarding the wavelength to start the photocatalytic oxidation of undoped TiO_2. However, the functional capability of the photocatalytic reaction seemed to be ensured even under VIS light as degradation ratios between 32 and 43% were obtained depending on the substrate. Moreover, one has to note that the low value of UV-A irradiance associated with VIS light condition tested in this study could be obtained in real-world conditions as shown by the UV light intensity monitoring campaign carried out in an indoor environment on cloudy days in Toulouse. Moreover, indoor UV irradiance could be improved by choosing the appropriate commercial lighting system.

This study shows promising results concerning the efficiency of TiO_2-based functional coatings to degrade NO providing some parameters such as the TiO_2 dry matter content on the surface, the substrate nature, and the illumination conditions are well defined. The authors want to highlight that further study on surface roughness characterization has to be carried out as it is a parameter of utmost importance for photocatalysis performance. Moreover, experiments with UV-filtered fluorescent lighting will be worth conducting.

Conflicts of Interest

The authors declare that there is no conflict of interest regarding the publication of this paper.

Acknowledgments

The authors are grateful to CRISTAL for providing photocatalytic products, to RENATECH French national nanofabrication network coordinated by CNRS for its expertise in confocal laser scanning microscopy, and to the French Government for its financial support for the DAIP project [61].

References

[1] J. Colls, *Air Pollution © 2002*, Spoon Press, London, 2nd Edition edition, 2002.

[2] S. Roy, M. S. Hegde, and G. Madras, "Catalysis for NOx abatement," *Applied Energy*, vol. 86, no. 11, pp. 2283–2297, 2009.

[3] European Parliament and Council of the European Union, "Directive 2008/50/EC of the European Parliament and of the Council of 21 May 2008 on ambient air quality and cleaner air for Europe," *Official Journal of the European Union*, vol. 51, 152 pages, 2008, http://data.europa.eu/eli/dir/2008/50/oj.

[4] WHO (World Health Organization), *WHO Air Quality Guidelines Global Update 2005*, Report on a WHO Working Group, Bonn, Germany, 2005.

[5] WHO (World Health Organization), *WHO Guidelines for Indoor air Quality: Selected Pollutants*, Working group meeting, Bonn, Germany, 2009.

[6] J.-M. Daisey, W.-J. Angell, and M.-G. Apte, "Indoor air quality, ventilation and health symptoms in schools: an analysis of existing information," *Indoor Air*, vol. 13, pp. 53–64, 2003.

[7] S. Kirchner, J.-F. Arènes, C. Cochet et al., "Campagne nationale logements : état de la qualité de l'air dans les logements français - Rapport final," CSTB-ANSES-OQAI. Report n° DDD-SB-2006-057, France, 2006, http://www.oqai.fr/userdata/documents/Document_133.pdf.

[8] S. Kirchner, A. Buchmann, C. Cochet et al., *Qualité d'air intérieur, qualité de vie : 10 ans de recherche pour mieux respirer*, CSTB Editions, France, 2011.

[9] P. Blondeau, V. Lordache, O. Poupard, D. Gerrin, and F. Allard, "Relationship between outdoor and indoor air quality in eight French schools," *Indoor Air*, vol. 15, pp. 2–12, 2005.

[10] A.-J. Lawrence, A. Masih, and A. Taneja, "Indoor/outdoor relationships of carbon monoxide and oxides of nitrogen in domestic homes with roadside, urban and rural locations in a central Indian region," *Indoor Air*, vol. 15, pp. 76–82, 2005.

[11] A. Folli, S.-B. Campbell, J.-A. Anderson, and D. Macphee, "Role of TiO2 surface hydration on NO oxidation photo-activity," *Journal of Photochemistry and Photobiology A: Chemistry*, vol. 220, pp. 85–93, 2011.

[12] A.-G. Agrios and P. Pichat, "State of the art and perspectives on materials and applications of photocatalysis over TiO2," *Journal of Applied Electrochemistry*, vol. 35, no. 7, pp. 655–663, 2005.

[13] M.-R. Hoffmann, S.-T. Martin, W. Choi, and D.-W. Bahnemann, "Environmental applications of semiconductor photocatalysis," *Chemistry Review*, vol. 95, pp. 69–96, 1995.

[14] F.-L. Toma, G. Bertrand, D. Klein, and C. Coddet, "Photocatalytic removal of nitrogen oxides via titanium dioxide," *Environmental Chemistry Letters*, vol. 2, no. 3, pp. 117–121, 2004.

[15] J.-S. Dalton, P.-A. Janes, N.-G. Jones, J.-A. Nicholson, K.-R. Hallam, and G.-C. Allen, "Photocatalytic oxidation of NOx gases using TiO2: a surface spectroscopic approach," *Environmental Pollution*, vol. 120, pp. 415–422, 2002.

[16] S. Devahasdin, C. Fan, K. Li, and D.-H. Chen, "TiO2 photocatalytic oxidation of nitric oxide: transient behavior and reaction kinetics," *Journal of Photochemistry and Photobiology A: Chemistry*, vol. 156, pp. 161–170, 2003.

[17] Y. Komazaki, H. Shimizu, and S. Tanaka, "A new measurement method for nitrogen oxides in the air using an annular diffusion scrubber coated with titanium dioxide," *Atmospheric Environment*, vol. 33, pp. 4363–4371, 1999.

[18] C.-M. Teh and A.-R. Mohamed, "Roles of titanium dioxide and ion-doped titanium dioxide on photocatalytic degradation of organic pollutants (phenolic compounds and dyes) in aqueous solutions: a review," *Journal of Alloys and Compounds*, vol. 509, pp. 1648–1660, 2011.

[19] R. Dillert, J. Stötzner, A. Engel, and D.-W. Bahnemann, "Influence of inlet concentration and light intensity on the photocatalytic oxidation of nitrogen (II) oxide at the surface of Aeroxide® TiO2 P25," *Journal of Hazardous Materials*, vol. 211, pp. 240–246, 2012.

[20] T. Martinez, A. Bertron, E. Ringot, and G. Escadeillas, "Degradation of NO using photocatalytic coatings applied to different substrates," *Building and Environment*, vol. 46, pp. 1808–1816, 2011.

[21] J.-V.-S. MeloDe and G. Trichês, "Evaluation of the influence of environmental conditions on the efficiency of photocatalytic coatings in the degradation of nitrogen oxides (NOx)," *Building and Environment*, vol. 49, pp. 117–123, 2012.

[22] R. Sugrañez, J.-I. Álvarez, M. Cruz-Yusta, I. Mármol, J. Vila, and L. Sánchez, "Enhanced photocatalytic degradation of NOx gases by regulating the microstructure of mortar cement modified with titanium dioxide," *Building and Environment*, vol. 69, pp. 55–63, 2013.

[23] M. Birnie, S. Riffat, and M. Gillott, "Photocatalytic reactors: design for effective air purification," *International Journal of Low Carbon Technologies*, vol. 1, no. 1, pp. 47–58, 2006.

[24] S. Ifang, M. Gallus, S. Liedtke, R. Kurtenbach, P. Wiesen, and J. Kleffmann, "Standardization methods for testing photo-catalytic air remediation materials: problems and solution," *Atmospheric Environment*, vol. 91, pp. 154–161, 2014.

[25] ISO 22197-1, *Fine Ceramics (Advanced Ceramics, Advanced Technical Ceramics) – Test Method for air Purification Performance of Semiconducting Photocatalytic Materials – Part 1: Removal of Nitric Oxide*, International Organization for Standardization, Geneva, Switzerland, 2016.

[26] A. Mills, C. Hill, and P.-K. Robertson, "Overview of the current ISO tests for photocatalytic materials," *Journal of Photochemistry and Photobiology A: Chemistry*, vol. 237, pp. 7–23, 2012.

[27] C. Minero, A. Bedini, and M. Minella, "On the standardization of the photocatalytic gas/solid tests," *International Journal of Chemical Reactor Engineering*, vol. 11, no. 2, pp. 717–732, 2013.

[28] XP B44-011, *Photocatalyse – Méthode d'essai pour l'évaluation des matériaux photocatalytiques vis-à-vis de la dégradation des NOx – Méthode à un seul passage en mode tangentiel*, AFNOR (Association Française de Normalisation), France, 2009.

[29] E. Boonen, V. Akylas, F. Barmpas, and A. Beeldens, "Construction of a photocatalytic de-polluting field site in the Leopold II tunnel in Brussels," *Journal of Environmental Management*, vol. 155, pp. 136–144, 2015.

[30] M. Chen and J. W. Chu, "NOx photocatalytic degradation on active concrete road surface—from experiment to real-scale application," *Journal of Cleaner Production*, vol. 19, no. 11, pp. 1266–1272, 2011.

[31] M. Gallus, V. Akylas, F. Barmpas et al., "Photocatalytic depollution in the Leopold II tunnel in Brussels: NOx abatement results," *Building and Environment*, vol. 84, no. 2, pp. 125–133, 2015.

[32] M. Gallus, R. Ciuraru, F. Mothes et al., "Photocatalytic abatement results from a model street canyon," *Environmental Science and Pollution Research*, vol. 22, no. 22, pp. 18185–18196, 2015.

[33] T. Maggos, J.-G. Bartzis, M. Liakou, and C. Gobin, "Photocatalytic degradation of NOx gases using TiO2-containing paint: a real scale study," *Journal of Hazardous Materials*, vol. 146, pp. 668–673, 2007.

[34] T. Maggos, J.-G. Bartzis, P. Leva, and D. Kotzias, "Application of photocatalytic technology for NOx removal," *Applied Physics A*, vol. 89, pp. 81–84, 2007.

[35] T. Maggos, A. Plassais, J. Bartzis, and L. Bonafous, "Photocatalytic degradation of NOx in a pilot street canyon configuration using TiO2-mortar panels," *Environmental Monitoring and Assessment*, vol. 136, pp. 35–44, 2008.

[36] J. Ângelo, L. Andrade, L.-M. Madeira, and A. Mendes, "An overview of photocatalysis phenomena applied to NOx abatement," *Journal of Environmental Management*, vol. 129, pp. 522–539, 2013.

[37] E. Boonen and A. Beeldens, "Recent photocatalytic applications for air purification in Belgium," *Coatings*, vol. 4, pp. 553–573, 2014.

[38] G.-L. Guerrini, "Photocatalytic performance in a city tunnel in Rome: NOx monitoring results," *Construction and Building Materials*, vol. 27, pp. 165–175, 2012.

[39] J. Hot, T. Martinez, B. Wayser, E. Ringot, and A. Bertron, "Photocatalytic degradation of NO/NO2 gas injected into a 10-m3 experimental chamber," *Environmental Science and Pollution Research*, vol. 24, no. 14, pp. 12562–12570, 2016.

[40] A. Fujishima and X. Zhang, "Titanium dioxide photocatalysis: present situation and future approaches," *Comptes Rendus Chimie*, vol. 9, pp. 750–760, 2006.

[41] M. Asiltürk, F. Sayılkan, and E. Arpaç, "Effect of Fe3+ ion doping to TiO2 on the photocatalytic degradation of malachite green dye under UV and vis-irradiation," *Journal of Photochemistry and Photobiology A: Chemistry*, vol. 203, pp. 64–71, 2009.

[42] C.-T. Hsieh, W.-S. Fan, W.-Y. Chen, and J.-Y. Lin, "Adsorption and visible-light-derived photocatalytic kinetics of organic dye on Co-doped titania nanotubes prepared by hydrothermal synthesis," *Separation and Purification Technology*, vol. 67, no. 3, pp. 312–318, 2009.

[43] G. Mailhot, M. Brigante, and K. Hanna, "Use and role of iron species in advanced oxidation processes," in *Plenary lecture at: 9th SPEA European Congress in Strasbourg, France*, 2016.

[44] L. Mai, C. Huang, D. Wang, Z. Zhang, and Y. Wang, "Effect of C doping on the structural and optical properties of sol-gel TiO2 thin films," *Applied Surface Science*, vol. 255, pp. 9285–9289, 2009.

[45] F. Peng, L. Cai, H. Yu, and J. Yang, "Synthesis and characterization of substitutional and interstitial nitrogen-doped titanium dioxides with visible light photocatalytic activity," *Journal of Solid State Chemistry*, vol. 181, no. 1, pp. 130–136, 2008.

[46] NF EN 196-1, *Methods of Testing Cement – Part 1: Determination of Strength*, AFNOR (Association Française de Normalisation), France, 2016.

[47] M. Faraldos, R. Kropp, M.-A. Anderson, and K. Sobolev, "Photocatalytic hydrophobic concrete coatings to combat air pollution," *Catalysis Today*, vol. 259, pp. 228–236, 2016.

[48] M.-Z. Guo, A.-M. Ramirez, and C.-S. Poon, "Self-cleaning ability of titanium dioxide clear paint coated architectural mortar and its potential in field application," *Journal of Cleaner Production*, vol. 112, pp. 3583–3588, 2016.

[49] M.-M. Hassan, H. Dylla, L.-N. Mohammad, and T. Rupnow, "Effect of application methods on the effectiveness of TiO2 as photocatalyst compound to concrete pavement," in *Transportation Research Board. 89th Annual Meeting, Washington D.C*, 2010.

[50] S. Shen, M. Burton, B. Jobson, and L. Haselback, "Pervious concrete with titanium dioxide as a photocatalyst compound for a greener urban road environment," *Construction and Building Materials*, vol. 35, pp. 874–883, 2012.

[51] M. M. Ballari and H. J. H. Brouwers, "Full scale demonstration of air-purifying pavement," *Journal of Hazardous Materials*, vol. 254–255, no. 1, pp. 406–414, 2013.

[52] C. Toro, B. T. Jobson, L. Haselbach, S. Shen, and S. H. Chung, "Photoactive roadways: determination of CO, NO and VOC uptake coefficients and photolabile side product yields on TiO2 treated asphalt and concrete," *Atmospheric Environment*, vol. 139, pp. 37–45, 2016.

[53] G. Hüsken, M. Hunge, and H.-J.-H. Brouwers, "Experimental study of photocatalytic concrete products for air purification," *Building and Environment*, vol. 44, no. 12, pp. 2463–2474, 2009.

[54] S. Karapati, T. Giannakopoulou, N. Todorova, N. Boukos, D. Dimotikali, and C. Trapalis, "Eco-efficient TiO2 modification for air pollutants oxidation," *Applied Catalysis B: Environmental*, vol. 176, pp. 578–585, 2015.

[55] S. Karapati, T. Giannakopoulou, N. Todorova et al., "Novel "Pickering" modified TiO2 photocatalysts with high De-NOx efficiency," *Catalysis Today*, vol. 287, pp. 45–51, 2017.

[56] L. Sivachandiran, F. Thevenet, P. Gravejat, and A. Rousseau, "Investigation of NO and NO2 adsorption mechanisms on TiO2 at room temperature," *Applied Catalysis B: Environmental*, vol. 142, pp. 196–204, 2013.

[57] M. Horgnies, I. Dubois-Brugger, and E. M. Gartner, "NOx depollution by hardened concrete and the influence of activated charcoal additions," *Cement and Concrete Research*, vol. 42, no. 10, pp. 1348–1355, 2012.

[58] N. Todorova, T. Giannakopoulou, S. Karapati, D. Petridis, T. Vaimakis, and C. Trapalis, "Composite TiO2/clays materials for photocatalytic NOx oxidation," *Applied Surface Science*, vol. 319, no. 1, pp. 113–120, 2014.

[59] A.-M. Ramirez, K. Demeestere, N. BelieDe, T. Mäntyla, and E. Levänen, "Titanium dioxide coated cementitious materials for air purifying purposes: preparation, characterization and toluene removal potential," *Building and Environment*, vol. 45, no. 3, pp. 832–838, 2010.

[60] E. Jimenez-Relinque, J.-R. Rodriguez-Garcia, A. Castillo, and M. Castellote, "Characteristics and efficiency of photocatalytic cementitious materials: type of binder, roughness and microstructure," *Cement and Concrete Research*, vol. 71, pp. 124–131, 2015.

[61] Guard Industrie, LMDC, LRVision, DAIP project, "Indoor air depollution by ahotocatalysis," 2012, Eco-Industries 2012 call for project, http://www.daip-depollution.com/en/.